Drop-Size Distribution Characteristics in Tropical Mesoscale Convective Systems

ROBERT CIFELLI

Joint Center for Earth Systems Technology, University of Maryland, Baltimore County, Baltimore, Maryland

CHRISTOPHER R. WILLIAMS, DEEPAK K. RAJOPADHYAYA, AND SUSAN K. AVERY

Cooperative Instititute for Research in Environmental Sciences, University of Colorado, Boulder, Colorado

KENNETH S. GAGE

NOAA Aeronomy Laboratory, Boulder, Colorado

P. T. MAY

Bureau of Research Meteorology Centre, Melbourne, Victoria, Australia

(Manuscript received 23 June 1998, in final form 4 June 1999)

ABSTRACT

Drop-size distribution characteristics were retrieved in eight tropical mesoscale convective systems (MCS) using a dual-frequency (UHF and VHF) wind profiler technique. The MCSs occurred near Darwin, Australia, during the 1993/94 wet season and were representative of the monsoon (oceanic) regime. The retrieved drop-size parameters were compared with corresponding rain gauge and disdrometer data, and it was found that there was good agreement between the measurements, lending credence to the profiler retrievals of drop-size distribution parameters. The profiler data for each MCS were partitioned into a three-tier classification scheme (i.e., convective, mixed convective–stratiform, and stratiform) based on a modified version of Williams et al. to isolate the salient microphysical characteristics in different precipitation types. The resulting analysis allowed for an examination of the drop-size distribution parameters in each category for a height range of about 2.1 km in each MCS.

In general, the distributions of all of the retrieved parameters showed the most variability in convection and the least in stratiform, with the mixed convective–stratiform category usually displaying intermediate characteristics. Although there was significant overlap in the range of many of the parameter distributions, the mean profiles were distinct. In the stratiform region, there was minimal vertical structure for all of the drop-size distribution parameters. This result suggests an equilibrium between depletion (e.g., evaporation) and growth (e.g., coalescence) over the height range examined. In contrast, the convective parameter distributions showed a more complicated structure, probably as a consequence of the complex microphysical processes occurring in the convective precipitation category.

Reflectivity–rainfall (Z–R) relations of the form $Z = AR^B$ were developed for each precipitation category as a function of height using linear regressions to the profiler retrievals of R and Z in log space. Similar to findings from previous studies, the rainfall decreased *for a given reflectivity* as the precipitation type changed from convective to stratiform. This result primarily was due to the fact that the coefficient A in the best-fit stratiform Z–R was approximately a factor of 2 greater than the convective A at all heights. The coefficient A *generally* increased downward with height in each category; the exponent B showed a small decrease (stratiform), almost no change (convective), or a slight increase (mixed convective–stratiform). Consequently, the amount by which convective rain rate exceeded stratiform (for a given reflectivity) varied significantly as a function of height, ranging from about 15% to over 80%.

1. Introduction

Accurate measurements of drop-size distributions are important for many meteorological applications, including estimation of rainfall, cloud radiative transfer studies, and cloud model initialization and verification. For example, McGaughey et al. (1996), Viltard et al. (1998), and McKague et al. (1998) all demonstrated the large sensitivity of passive microwave algorithms to the prescribed drop-size distribution in both convective and stratiform rain precipitation. Recent numerical modeling studies have demonstrated large sensitivity in terms of

Corresponding author address: Dr. Robert Cifelli, Department of Atmospheric Science, Colorado State University, Fort Collins, CO 80523. E-mail: rob@olympic.atmos.colostate.edu

surface rainfall production, evaporation, and downdraft intensity to the parameterized hydrometeor size distribution below the melting level, especially in tropical mesoscale convective systems (MCS; Ferrier et al. 1995). Drop-size distributions in clouds are difficult to observe directly. These measurements are typically recorded using probes mounted on aircraft. The observations are limited to the regions where the planes fly, thus producing sporadic measurements in time and space (e.g., Rogers et al. 1993). Moreover, the sample volume is typically small so that it may not always be possible to obtain representative drop-size distributions (e.g., Richter and Hagen 1997).

Scanning Doppler radars, operating at microwave frequencies, have traditionally been used to sense clouds remotely and to study drop-size distributions. Direct estimation of the drop-size distribution using vertically pointing radars have been attempted in many previous studies; however, because of the fact that the drop-size distribution is affected by vertical air motions, these methods are limited to regions where the vertical draft structure is well known or can be neglected (Rogers 1967; Atlas et al. 1973; Atlas et al. 1995). A common technique for radar estimation of rainfall is to develop relationships between the backscattered energy return to the radar (i.e., reflectivity Z) and rainfall (R). Both Z and R are dependent on the drop-size distribution through the following relations:

$$R = \frac{\pi}{6} \int_0^\infty N(D) D^3 V(D)\, dD \quad \text{and} \tag{1}$$

$$Z = \int_0^\infty N(D) D^6\, dD, \tag{2}$$

where $N(D)$ is the drop-size distribution, D is the drop diameter, and V is the fall velocity of the drop. The Z–R technique has the advantage of producing rainfall estimates over large areas [$O(50\ 000\ \text{km}^2)$] in relatively short time (several minutes). Unfortunately, the existence of various range-dependent errors can produce significant biases in the scanning radar estimate of rainfall (e.g., Wilson and Brandes 1979; Zawadzki 1984; Austin 1987). Moreover, many previous observational studies have shown that natural variations of the drop-size distribution in time and space can lead to different Z–R parameterizations, ultimately producing different estimates of rain rates (e.g., Battan 1973; Ulbrich 1983; Austin 1987; Huggel et al. 1996).

Unlike scanning radars, wind profilers routinely sample in the vertical direction within a relatively small spatial domain, allowing them to resolve small-scale variations in the vertical air motion (VHF) and precipitation (UHF) patterns and avoiding many of the range-dependent errors inherent in traditional scanning radar estimate of rainfall. Moreover, the profilers can operate with minimum attention for relatively long periods so that climate statistics of the drop-size distribution and kinematic parameters can be developed for a given area. Because the profiler can observe the evolution of the drop-size distribution with relatively high vertical resolution, these instruments have the potential to serve as calibration tools for scanning radar estimates of surface rainfall using empirical Z–R relations.

A number of recent studies have examined the applicability of separate Z–R relations for convective and stratiform rain. Short et al. (1990) and Tokay and Short (1996) have shown, using disdrometer data from Darwin, Australia, and the tropical western Pacific, that the drop-size distribution undergoes abrupt shifts between convective and stratiform precipitation and that rainfall rates are improved when two Z–R relations are used instead of one. However, Steiner and Houze (1997) showed that the use of two Z–R relations instead of one did not significantly improve monthly rain totals using radar data at Darwin, Australia. Also, Yuter and Houze (1997) have argued that convective and stratiform drop-size distributions in the tropical western Pacific are not statistically distinct. Clearly, more research on the variability of the drop-size distribution in different precipitation regimes is required.

This paper takes a step in that direction by reporting on results of drop-size distribution retrievals using dual-frequency (UHF and VHF) wind profiler measurements. The retrieved distributions are classified into separate precipitation categories based on a modified version of Williams et al. (1995) in order to examine differences in microphysical structure for each precipitation category. The retrievals are performed over a 2.1-km depth, starting at 1.6 km and extending upward to 3.7 km (approximately 1.0 km below the 0°C isotherm). The drop-size distribution results are used to develop Z–R relations in each precipitation category. The results of this study show that, despite large overlap in the distribution of the drop-size parameters, significant differences occur in the mean Z–R parameterization for each category as a function of height.

A recent study by McKague et al. (1998) also reported results of the profiler retrieval method on Darwin data. However, in that study, the authors examined the sensitivity of a microwave radiative transfer model to variations in the drop-size spectra. No attempt was made to examine the vertical variability of the drop-size distribution in different precipitation regimes.

A description of the dual-frequency retrieval technique and the precipitation classification scheme is provided in section 2. In section 3, comparisons of the retrieved rain totals and rain gauge data are presented as is a statistical comparison of the profiler-estimated mean volume diameter with corresponding disdrometer measurements. The differences in the drop-size distribution in each precipitation category are also discussed. Last, this section includes a discussion of the effect of drop-size distribution variations on Z–R parameterizations. Some closing remarks are presented in section 4.

TABLE 1. Relevant UHF and VHF profiler parameters.

Radar parameter	UHF value	VHF value
Wavelength (m)	0.33	6.02
Peak power (kW)	~0.5	~30
3-dB beamwidth (%)	~9	~3
Pulsewidth (ns)	700 (low)	3300
Interpulse period (s)	3300 (high)	
	51 (low)	400
	142 (high)	
Number of coherently integrated points	107 (low)	250
	38 (high)	
Number of spectral averages	70 (low)	3
	35 (high)	
Nyquist velocity (m s^{-1})	15	15
Number of range gates	60	70
Lowest range gate (m)	120 (low)	1595
	105 (high)	
Range gate spacing (m)	105 (low)	300
	300 (high)	
Update time on vertical beam (min)	1.67	2.50

2. Methodology

The Darwin area is located at the southern tip of the maritime continent (12°S, 131°E) and has a pronounced monsoon climate with the majority of rainfall received between November and March. This area also has an extensive set of meteorological instrumentation in support of the Tropical Rainfall Measuring Mission (TRMM) (Simpson et al. 1988) program. During the 1993/94 wet season, the Bureau of Research Meteorology Centre (BMRC) VHF- and the NOAA Aeronomy Laboratory (AL) UHF profilers were collocated at the Darwin field site and operated in a nearly identical sampling mode (described below). An NOAA AL tipping bucket rain gauge was also located at the field site to compare with the profiler measurements.

a. Sampling strategy

The wind profiler is a Doppler radar with fixed antenna beams at or near zenith. The characteristics of the UHF and VHF profilers used in this study are shown in Table 1. During the 1993/94 wet season, both the UHF and VHF profilers were alternately sampling the vertical and off-vertical beams. In addition, the UHF profiler operated in two separate height resolution modes: ''high'' height mode and ''low'' height mode (Carter et al. 1995; see Table 1). For this study, only data from the high height mode are used. The update time on the vertical beam was approximately 100 s for the UHF and 150 s for the VHF profiler. Moreover, the range gates were not precisely matched; thus, a linear interpolation scheme was used in space and time to match the VHF and UHF data.

b. Retrieval algorithm

Techniques for retrieving raindrop-size distributions using wind profiler data have been developed over the past decade (Wakasugi et al. 1986; Gossard 1988; Rajopadhyaya et al. 1993; 1998; Currier et al. 1992; Maguire and Avery 1994). The limitations and sources of error in these techniques have been examined and data have been ''ground truthed'' against in situ aircraft measurements (Rogers et al. 1993), disdrometers (McKague et al. 1998), and rain gauge measurements (Rajopadhyaya et al. 1998).

In this study, a spectra-fitting algorithm is used to retrieve both the vertical air motions (VHF) and the hydrometeor-size distribution parameters (UHF) from the wind profiler data. The general procedure to retrieve the drop-size distribution from combined 50 and 915 MHz profiler spectra is described in Maguire and Avery (1994) and McKague et al. (1998) and only a brief summary will be provided here. The model takes advantage of the different scattering sensitivities of UHF and VHF to precipitation and ''clear air.'' At VHF, the wind profiler has approximately equal sensitivity to Bragg scatter from gradients in the clear air index of refraction (i.e., turbulence) and Rayleigh scatter from precipitation targets. In contrast, the UHF profiler is dominated by Rayleigh scatter whenever the precipitation exceeds light rain or drizzle (e.g., Ralph 1995).

The model uses a Gaussian distribution to fit the power spectra in the VHF data, extract the vertical air velocity information (i.e., mean vertical air motion and spectral width), and to isolate the portion of the spectra associated with precipitation scatter. The model then examines the UHF data to fit the precipitation component of the spectra with an assumed functional form (i.e., Gaussian, lognormal, gamma, exponential) for the drop-size distributions. A least squares fitting routine minimizes chi square (χ^2) values in order to obtain a best fit to the observed Doppler spectra by varying N_0, μ, and Λ. In this study, we use a gamma distribution of the form

$$N(D) = N_0 D^{\mu} e^{(-\Lambda D)}, \tag{3}$$

where D is the drop diameter and N_0, μ, and Λ are the amplitude, shape parameter, and slope of the distribution. Maximum drop size used in the fitting procedure is 6 mm. Resolution of small drops depends on the spectral width of the vertical air velocity (Rajopadhyaya et al. 1998); however, it is anticipated to be on the order of 0.5 mm or less based on tests with simulated data. The median volume diameter D_0 is determined from the relationship

$$\Lambda D_0 = 3.67 + \mu. \tag{4}$$

Because the precipitation backscatter observed with the wind profiler is smeared by the clear air, it is essential to obtain an accurate estimate of turbulence parameters for the retrieval of the drop-size distribution (e.g., Rajopadhyaya et al. 1998). Once the drop-size distribution parameters have been retrieved, other moments of the

TABLE 2. Summary of stacked spectra profiles analyzed for each rainfall event. Each profile contains retrievals from eight range gates extending from 1.6–3.7 km.

Event date (YY yearday)	Total hours of observation	No. of stacked spectra profiles analyzed
93347	4.5	150
93353	2.0	60
93359	1.8	53
93362	16.0	563
94007	4.0	132
94046	7.5	257
94056	4.5	150
94068	2.5	78
Total	42.8	1443

drop-size distribution (e.g., reflectivity[1], liquid water content, and rain rate) can be calculated in a straightforward manner.

The height range of the retrieval analysis is limited from below by the distance to the first VHF range gate (1.6 km) and above by ice contamination below the 0°C isotherm. For the Darwin MCSs examined, it was found that the retrievals were sometimes corrupted, presumably by ice contamination, at distances within 0.8 km of the 0°C level. Therefore, we restrict our analysis to a maximum height of 3.7 km (about 1 km below the melting level). For each profiler vertical beam sample, retrievals were performed on all range gates extending from 1.6 to 3.7 km. We hereinafter refer to each vertical beam sample (each containing retrievals for 8 range gates) as a stacked spectra profile. Table 2 lists the total number of stacked spectra profiles analyzed for each MCS event.

Details in the potential sources of error in the retrieval model are provided in McKague et al. (1998) and Rajopadhyaya et al. (1998). Both of these studies point out the sensitivity of the retrieval to correct measurement of the vertical air motion in the VHF data. The estimated retrieval error in the median volume diameter is on the order of 20%. Although the retrievals estimate D_0 well, the shape parameter has large errors arising from the low-reflectivity contribution of small drops. Thus, the turn over of the drop-size distribution at small sizes is not accurately measured, particularly when combined with errors in correction for vertical air motion spectral width and mean Doppler shift. Also, sensitivity tests with simulated data showed that drop-size distribution retrievals were unreliable when the shape parameter became large (McKague et al. 1998; Rajopadhyaya et al. 1998). Therefore, the shape parameter was constrained to be a maximum of 9.0 in the retrieval algorithm.

In this study, only retrievals that meet a specific set of rigid criteria are used in the analysis of drop-size distribution characteristics. Specifically, statistics of the drop-size distribution are examined for which the following criteria are met at *all* eight range gates[2] between 1.6 and 3.7 km:

1) the radar signal to noise exceeds 5,
2) the resulting chi square goodness of fit statistic is less than a specified threshold,
3) D_0 is less than 4.0 mm, and
4) the retrieved rain rate is at least 0.5 mm h^{-1} and less than 300 mm h^{-1}.

c. Classification of retrieved spectra

The profiler retrievals for the MCS were partitioned into a three-tier classification scheme (i.e., convective, mixed convective–stratiform—hereinafter referred to as mixed, and stratiform) following a modified version of Williams et al. (1995) in order to isolate the microphysical characteristics in different precipitation types. The three-tier classification was chosen instead of more traditional two-tier schemes (i.e., convective and stratiform) because previous studies have noted that significant portions of oceanic MCSs in the vicinity of Darwin and in the western Pacific commonly contain characteristics that are intermediate between convective and stratiform during their lifecycle, based on airborne Doppler radar studies (Mapes and Houze 1993, 1995).

The Williams et al. (1995) algorithm uses properties of the first and second moment (i.e., Doppler velocity and spectral width) of UHF profiler spectra to classify precipitation into four categories:

1) shallow convective,
2) deep convective,
3) mixed convective–stratiform, and
4) stratiform.

Note that the Williams et al. (1995) classification is based on the vertical structure of the spectral moment data at and above the melting level. The subsequent drop-size retrievals are performed at altitudes below the melting level. Specific parameters used in the algorithm include: the gradient of particle fall speed *near* the melting level; the reflectivity weighted spectral width *above* the melting level; and the presence of valid radar returns above the melting level. In this study, the Williams et al. (1995) algorithm has been modified in two ways: 1) shallow and deep convective are combined into a single convective category, and 2) vertical air motion spectral width (VHF) is incorporated into the classification algorithm in order to minimize spurious classification of convective spectra as described below. The first change has relatively minor effect, because all of the events

[1] Reflectivity can be calculated when the radar calibration factors are known (Maguire and Avery 1994).

[2] These criteria were not applied when comparing the profiler-retrieved rain total with the rain gauge in section 3a or in the time series of retrieved parameters discussed in section 3b.

TABLE 3. Number of stacked spectra profiles for each precipitation category that passed threshold criteria at all nine range gates.

Precipitation category	No. of stacked spectra profiles passing threshold criteria	Percent of available profiles rejected
Convective	70	45
Mixed	471	23
Stratiform	484	28

analyzed occurred during the passage of MCSs and are dominated by deep cloud. The latter modification was included in order to help to minimize the possibility of a spurious melting layer signature in the vertical beam Doppler velocity data. In the Williams et al. (1995) routine, the major threshold used to separate convective from mixed or stratiform is the occurrence of a melting layer signature defined by the presence of a particle fall speed gradient >2 m s^{-1} km^{-1} in the vicinity of the melting layer (3.4–5.2 km at Darwin) in the UHF data. This classification procedure was developed for profiler Doppler spectra that were averaged over a period of 30 min. In this study, individual spectra (each with a dwell time of 60 s) were utilized in the classification algorithm without averaging. For the unaveraged spectra, it was sometimes noted during the observation of convective cores that a relatively large Doppler fall velocity gradient occurred within the melting layer zone without any corresponding radar brightband signature. Detailed analyses showed that the large vertical gradient of hydrometeor fall speed (i.e., >2.0 m s^{-1} km^{-1}) were artifacts produced by correspondingly large vertical gradient of vertical air velocity (e.g., updraft superimposed on a downdraft or vise versa). The effect was most pronounced in the mixed category.[3] Thus, the vertical air motion information from the VHF profiler was used to help to eliminate the ambiguity. Following Cifelli and Rutledge (1998), any retrieval with a corresponding vertical air motion spectral width exceeding 1.2 m s^{-1} was automatically classified as convective and did not receive further algorithm discrimination processing. As shown in section 3b, the classification produced results consistent with previous studies of tropical MCSs.

Table 3 shows the total number of stacked spectra profiles used for statistical analysis in each precipitation category for all of the MCS events. Note that the actual number of profiles used in the analysis was smaller than the total number of available profiles (compare Tables 2 and 3). The difference is due to the strict criteria used to evaluate the retrievals. Recall that the thresholds reported above must be met at all eight range gates between 1.6 and 3.7 km for the results at any particular range gate to be utilized. The rigid criteria produced a significant reduction in the number of stacked spectra profiles available for analysis, especially in the convective category (see Table 3). Tests showed that the statistical results in the mixed and stratiform categories (described below in section 3) were relatively insensitive to the number of range gates exceeding the threshold criteria. However, in the convective category, some of mean profiles of the parameter distributions were sensitive to the number of range gates exceeding the threshold criteria. There was only a minor effect on the mode of each convective parameter distribution. The requirement of retrievals at all eight range gates passing the criteria likely eliminated many of the retrievals in the most intense convection situations and biased the results toward weak convection. However, this procedure ensured that only the most reliable retrievals were used and eliminated potential bias by incorporating different sample sizes at each height.

3. Results

a. Profiler-retrieved versus gauge rainfall accumulation

A comparison of rainfall totals for each MCS event was made between the profiler retrieval method and the surface tipping bucket rain gauge at the profiler site. Figure 1 shows a scatter diagram of the profiler-retrieved rainfall at 1.6 and 1.9 km (the lowest two range gates where the dual-frequency method could be applied) and corresponding rain gauge totals for all eight events used in this study. Also shown in the figure is the one-to-one line where all the points would line up if the gauge and profiler measurements agreed perfectly. Note that the profiler method underestimates in comparison with the gauge in some events and overestimates in others. The linear regression results show that the slope of the best-fit line is somewhat less than unity (0.73 at 1.6 km and 0.82 at 1.9 km) but the measurements are well correlated ($R = 0.96$–0.97). Rajopadhyaya et al. (1998) showed that the retrieved rainfall at 1.9 km from one particular MCS event (also used in this study) agreed well with the corresponding surface rain gauge measurement in terms of both the total accumulation and short-term variability of rain rate in both heavy and light rain conditions. Given the fact that the profiler and rain gauge measurements are collected at widely different sample sizes (roughly 7 orders of magnitude in sampling size area) and locations (ground surface versus 1.6–1.9 km), and that there are a large number of data gaps in the profiler data because of the sampling sequence between the vertical and oblique beams, the measurements are in reasonable agreement. In section 3b, we will show detailed comparisons between the rain gauge and profiler retrieval for one particular event.

b. Time series of precipitation characteristics for one MCS event

Figure 2 shows a time series analysis of several profiler-retrieved parameters (at a height of 1.9 km) from

[3] A similar effect was observed in the analysis of UHF profiler data from the tropical western Pacific region (Tokay et al. 1999).

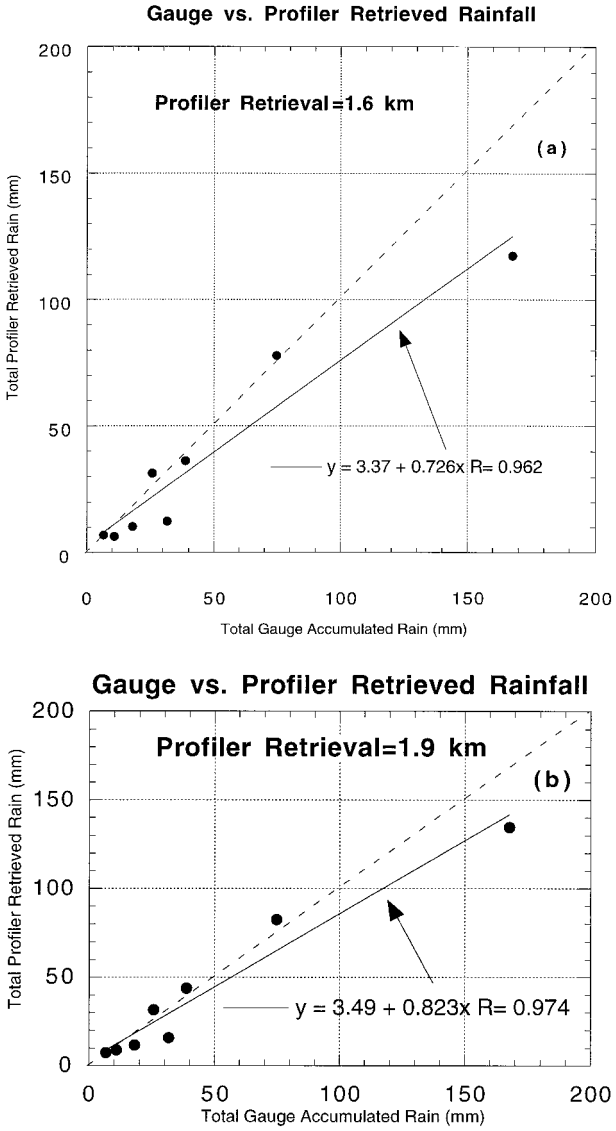

FIG. 1. Scatterplot of total profiler retrieved rain vs total tipping bucket gauge accumulated rainfall for the eight MCS events. The solid line indicates the best fit to the data using a linear regression technique and the dashed line indicates a perfect 1:1 correspondence between the measurements. The resulting best-fit line equation is also shown. Plot (a) is for retrieval data at 1.6 km and plot (b) is for retrieval data at 1.9 km.

one of the MCSs. Note that the total number concentration (N_T) is plotted in the top panel of Fig. 2 instead of the intercept parameter (N_0) in order to avoid ambiguities in interpretation due to the functional relationship between (N_0) and (μ) (Chandrasekar and Bringi 1987). Also shown in Fig. 2 is a time–height cross section of reflectivity factor, calculated using the zeroth-moment estimate of equivalent reflectivity (dBZ_e; Williams et al. 1995). Note that, because the zeroth moment is based on the integrated signal-to-noise ratio in the Doppler spectra and not on the retrieval of the drop-size distribution, this quantity can be derived above the freezing level, assuming the radar constant is known. The precipitation classification is also overlaid in each panel of Fig. 2 in order to illustrate the algorithm performance for this event.

The MCS shown in Fig. 2 is characterized by the passage of several convective cells, followed by the development of a radar bright band over the profilers. There is a significant amount of high-frequency variability in the retrieved median volume diameter (D_0), total number concentration (N_T), and rain rate, especially during the passage of vigorous convective cells (0445–0515 UTC and 0535–0600 UTC); however, the inverse correlation between D_0 and N_T is apparent throughout the event[4]. By approximately 0630 UTC, the precipitation shifts to mixed and stratiform. Note that the high-frequency variability of all the retrieved parameters is reduced after this time. The overall magnitude D_0 (N_T) begins to slowly increase (decrease) after about 0648 UTC, in association with the development of a radar brightband signature. Although there are visible trends in the retrieved parameters shown in Fig. 2 [e.g., the increase (decrease) in D_0 (N_T) during the heavy rain periods], it is also evident that there is a significant amount of overlap in each precipitation category. This feature will be discussed further in the next section.

Overall, the discrimination algorithm appears to do a reasonable job at classifying the precipitation in this MCS. The intense convective cells and associated high rain rates are classified as convective, and intermediary (decaying) cells are identified as mixed. The region containing the radar bright band is stratiform. The model-versus-rain gauge intensity plot in Fig. 2b shows that the two sets of measurements are in good agreement at times and not so good agreement at other times. In general, the two sets of measurements are better correlated at the lower rain rates. There are numerous reasons to expect differences between the instantaneous rain intensity measurements (e.g., wide disparity in sampling resolution and sampling location). It should also be noted that the degree of agreement between the profiler and rain gauge varied from one event to another [see Rajopadhyaya et al. (1998) for an example of excellent agreement at all rain intensities].

c. Comparison with disdrometer measurements

Another independent measure of validation of the profiler-estimated drop-size parameters is provided by comparing the measurements to corresponding disdrometer data (McKague et al. 1998). As described in the McKague et al. study, an impact disdrometer (Joss and Waldvogel 1967), located 3.5 km from the profiler site, collected independent drop-size distribution data during

[4] Because the profiler retrievals shown in Fig. 2 were not required to pass the rigid criteria discussed in Sec. 2, it is possible that some of the high-frequency variability in the time series may be anomalous.

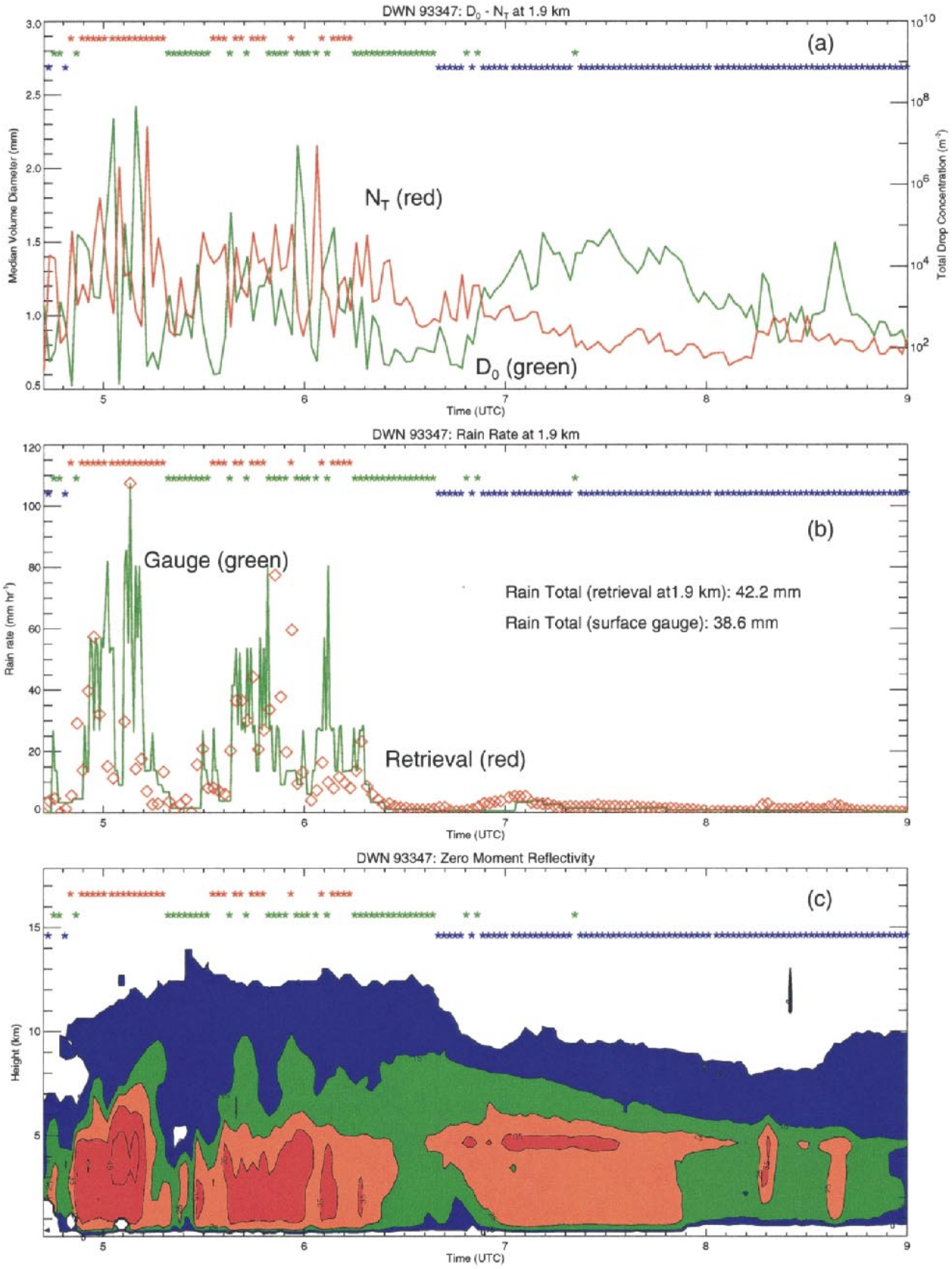

the 1993/94 wet season. The disdrometer data were sorted into 20 drop-diameter bins ranging in size from 0.35 to 5.0 mm and above prior to fitting the data using both least square and moment method techniques (McKague et al. 1998). Figure 3 shows histograms of D_0 at the lowest gate of profiler retrievals (1.6 km) as compared with the surface-based estimates of D_0 from the disdrometer (method of moments). Comparison of the plots in Fig. 3 shows that the distributions have the same mode (~1.2 mm). Moreover, the overall shapes of the profiler and disdrometer distributions are surprisingly similar, given the spatial separation (vertical and horizontal) as well as the large differences in sample resolution between the profiler and disdrometer. The agreement between the plots shown in Fig. 3 provides an additional degree of confidence in the profiler-retrieval methodology and suggest that the profiler retrievals can provide reliable information regarding the MCS drop-size distribution characteristics.

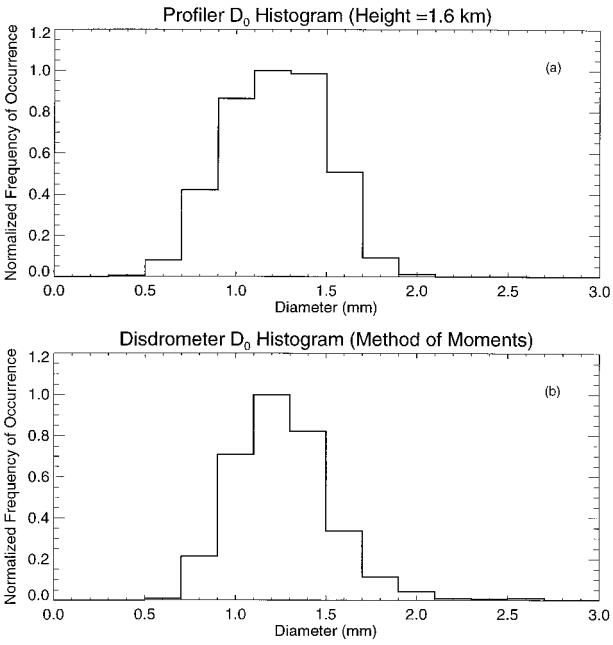

FIG. 3. Normalized histograms of median volume diameter (D_0) from (a) the profiler retrieval at 1.6 km and (b) the surface-based disdrometer using the method of moments. The profiler histogram includes data from all categories of precipitation that exceeded the criteria specified in the text. The disdrometer data are from McKague et al. (1998). Both histograms were generated using a bin size of 0.2 mm starting at 0.0 mm. Details of the disdrometer data analysis are provided in McKague et al. (1998).

d. Characteristics of retrieved parameters in each precipitation regime

In this section, we examine the vertical structure of profiler-retrieved parameters for all eight MCS events. As noted in section 2, the height range of the profiler retrievals extends over a 2.1-km depth, beginning at 1.6 km and extending upward to 3.7 km. Plots of each parameter are presented in CFAD (Contoured Frequency by Altitude Diagram) (Yuter and Houze 1995) format with the mean profile overlaid. Such displays are useful not only for determining changes in the parameter distribution width with height but also for providing some measure of the skewness.

The stratiform parameter distributions of vertical air motion (W), terminal fall speed (V_T, calculated as the difference between VHF-retrieved vertical motion and the UHF reflectivity-weighted particle fall speed), median volume diameter (D_0,) rain rate (R), liquid water content (LWC), reflectivity (Z), intercept parameter (N_0), and shape parameter (μ) are shown in Fig. 4. Note that the mean and mode are nearly collocated for almost all of the parameter distributions and that there is little apparent vertical variability (with the exception of N_0). However, as will be shown in section 3e, the changes with height, though small, have important consequences for Z–R parameterizations. The salient features of Fig. 4 are described below.

The stratiform W distribution (Fig. 4a) shows weak descending motion below the melting level, consistent with previous studies of MCS stratiform regions (e.g., Houze 1989). The terminal fall speed plot (Fig. 4b) shows an approximate linear decrease in V_T with decreasing height, nearly coincident with the increase in atmospheric density. This suggests that the particles are not undergoing significant size changes over the 2.1-km height range. The D_0 distribution (Fig. 4c) is fairly broad (nearly bimodal above 3 km) and, consistent with the V_T plot, the mode of D_0 is approximately constant throughout the 2.1 km depth. The magnitude of the D_0 mean profile (~1.2 mm) compares well to a previous study of a tropical squall line using VHF profiler data and a different retrieval technique (May and Rajopadhyaya 1996). The slight increase in dBZ with decreasing height (~1 dB; Fig. 4e) is again consistent with increasing atmospheric density and the resulting raindrop convergence.

Note that both R and LWC are also nearly constant with height (Figs. 4d and 4f). These results are in agree-

←

FIG. 2. Profiler observations during the passage of an MCS on 13 Dec 1993. Top panel (a) shows a time section of N_T (red line) and D_0 (green line) at 1.9 km using the dual-frequency profiler retrieval technique. Here, N_T is calculated from N_0 according to Chandrasekar and Bringi (1987). Middle panel (b) shows the corresponding retrieved rain rate at 1.9 km (red) and the surface rain gauge measurements (green). Bottom panel (c) shows a corresponding time–height section of equivalent reflectivity (dBZ_e) using the zeroth-moment data from the profiler Doppler spectra. In all three panels, the results of the precipitation classification are overlaid with a (*) symbol: red = convective, green = mixed, and blue = stratiform.

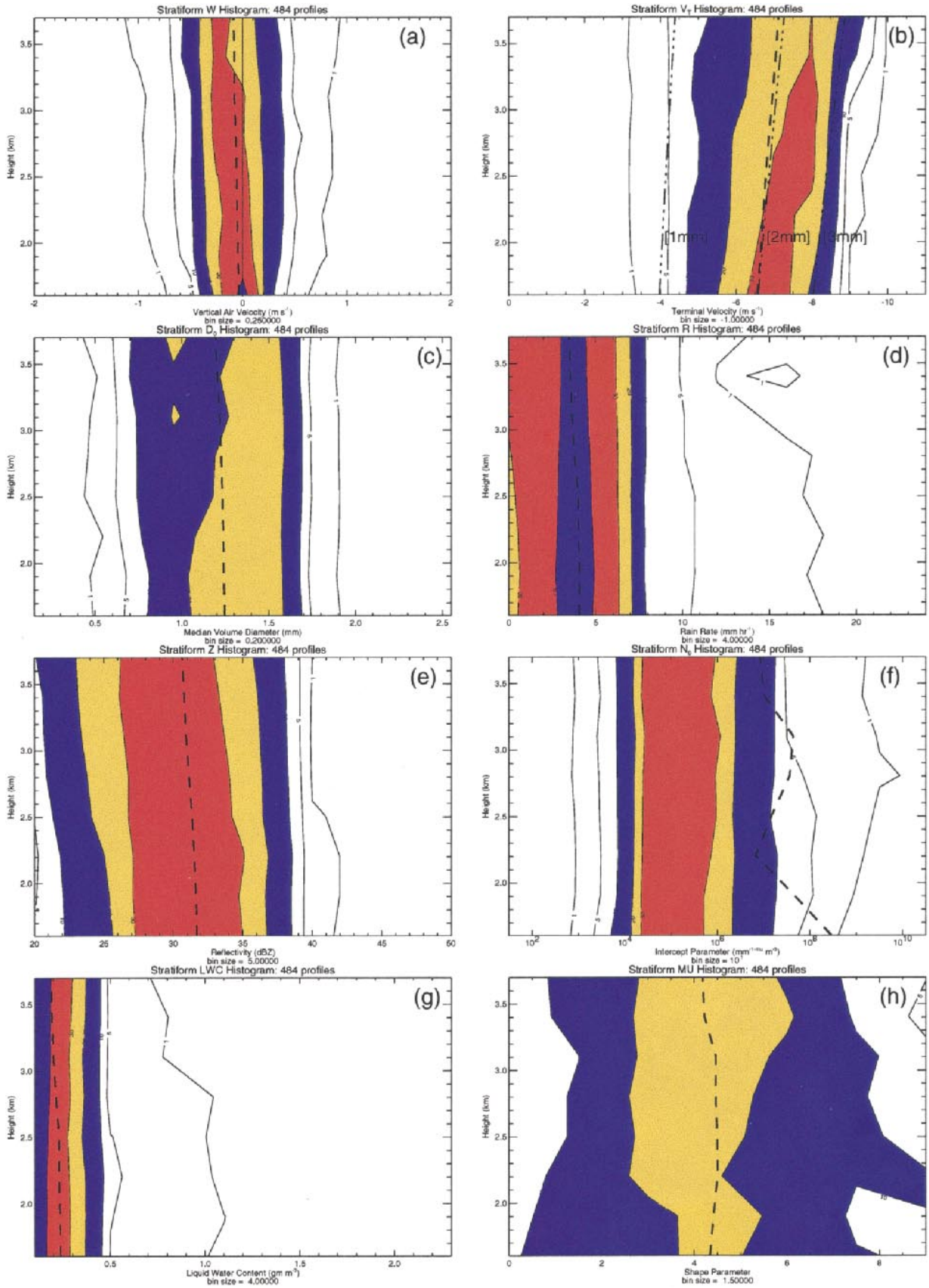

ment with Atlas et al. (1999). In that study, the authors used a combination of wind profiler and disdrometer data sampled from a tropical west Pacific MCS to show that Doppler fall speed and reflectivity remained relatively constant in the 2.0–3.5 km height range. However, significant changes in these parameters occurred below 2.0 km, which the authors' ascribed to evaporation. Numerical modeling experiments of tropical MCSs also suggest that evaporation has the largest effect below 2 km (Ferrier et al. 1995, 1996). It should be pointed out that the liquid water content results for stratiform rain in this study are somewhat at odds with a previous VHF wind profiler analysis of a tropical continental squall line sampled near Darwin (May and Rajopadhyaya 1997). In that study, the authors found a significant decrease in liquid water content in the 2.0- to 4.0-km height range, which the authors attributed to evaporation. The reason for the differences is not clear but may be due to the fact that the continental environment observed by May and Rajopadhyaya (1997) was drier and more conducive to evaporation than in the current events, which are representative of oceanic MCSs. The differences may also be due to the analysis techniques utilized in each study. In contrast to the dual-frequency approach employed here, May and Rajopadhyaya (1997) used VHF profiler data only. Because the sensitivity to small drops is more limited at VHF as opposed to UHF, their retrieval technique may not have been able to resolve the contribution from small drops.

The mode of the N_0 distribution (Fig. 4f) shows a slight decrease with height; however, there are significant fluctuations in the N_0 mean value due to the large variability of a few outliers. The shape parameter μ (Fig. 4h) is nearly constant over the height range of the profiler retrievals. The value of about 4 indicates that the stratiform drop-size distributions are somewhat narrower than expected from an exponential distribution (i.e., $\mu = 0$). Both the N_0 and μ stratiform results are consistent with similar surface disdrometer estimates in tropical rain for rain rates <20 mm h^{-1} (Tokay and Short 1996). Taken together, the results in Fig. 4 indicate minimal variation in the stratiform drop-size distribution, suggesting an approximate equilibrium between growth (i.e., coalescence) and decay (i.e., breakup and evaporation) processes over the 2.1-km depth in these MCSs.

The corresponding convective parameter distributions are shown in Fig. 5. Comparison of Figs. 4 and 5 shows that there is significant overlap in the convective and stratiform parameters. However, close inspection of these figures illustrate some important differences in drop-size distribution characteristics. In contrast to the stratiform region, the retrieved parameter distributions in the convective category are wider and show more vertical structure, suggesting a more complicated role of microphysical processes. This is not surprising, given the higher turbulence and mixing with resulting large variability in convective cells as opposed to widespread stratiform rain (recall the high-frequency variability of retrieved parameters shown in Fig. 2). Although rigid criteria were used to eliminate spurious retrievals, it is also possible that part of the variability of the convective parameters are due to increased spectral width of W and resulting retrieval errors in this precipitation category.

The convective W plot (Fig. 5a) shows a much more heterogeneous pattern compared to the corresponding stratiform plot, as evidenced by the relatively large width of the vertical air motion distribution over the 2.1-km height range. The resulting turbulence from the superposition of updrafts and downdrafts would be expected to give rise to a more complex drop-size distribution structure. The mean W is less than 1 m s^{-1}. As discussed in section 2, the implementation of the strict threshold criteria may be biasing the sample in this precipitation category toward weak convection. However, Cifelli and Rutledge (1998) and May and Rajopadhyaya (1999) have shown that monsoon MCSs in the vicinity of Darwin tend to have low mean W below the freezing level and the largest vertical drafts in the middle-to-upper troposphere. Mean vertical air motion data above the freezing level for the events examined herein (not shown) are consistent with these previous studies. In terms of V_T, the mode of the convective fall speeds are $\sim$1 m s^{-1} lower than in the stratiform distributions (Figs. 5b and 4b). Moreover, the decrease in V_T with decreasing height is much more pronounced in the stratiform category, suggesting that the density effect is counterbalanced by some microphysical growth process in the convective category. Similar results were observed over Manus Island in the tropical western Pacific using UHF-only profiler observations of convective precipitation (Williams et al. 1995; Tokay et al. 1998).

The mode of the convective D_0 (Fig. 5c) is slightly smaller ($\sim$0.25 mm) above 2 km and increases with decreasing altitude in comparison with the corresponding stratiform plot (Fig. 5c). Note that the modes of the convective R and Z plots (Figs. 5d and 5e, respectively) are nearly identical to their stratiform counterparts. However, the mean convective R and Z profiles are larg-

←

FIG. 4. Contoured frequency by altitude diagram (CFAD) retrieved parameters for the stratiform precipitation category of (a) vertical air motion, W, (b) terminal fall speed, V_T, (c) median volume diameter, D_0, (d) rain rate, R, (e) reflectivity, Z, (f) intercept parameter, N_0, (g) liquid water content, LWC, and (h) shape parameter, MU. Units for each parameter are shown at the bottom of the corresponding plot. Contours indicate relative frequency of occurrence at each height, with blue, yellow, and red shading indicating $\geq$10%, 20%, and 30%, respectively. The mean profile for each distribution is indicated as a dashed line. The total number of profiles composing each CFAD and the bin size are indicated in each plot. The dash–dot lines in the V_T plot indicate the expected change in fall speed with height due to increasing density for a 1-, 2-, and 3-mm drop [calculations following Beard (1985)].

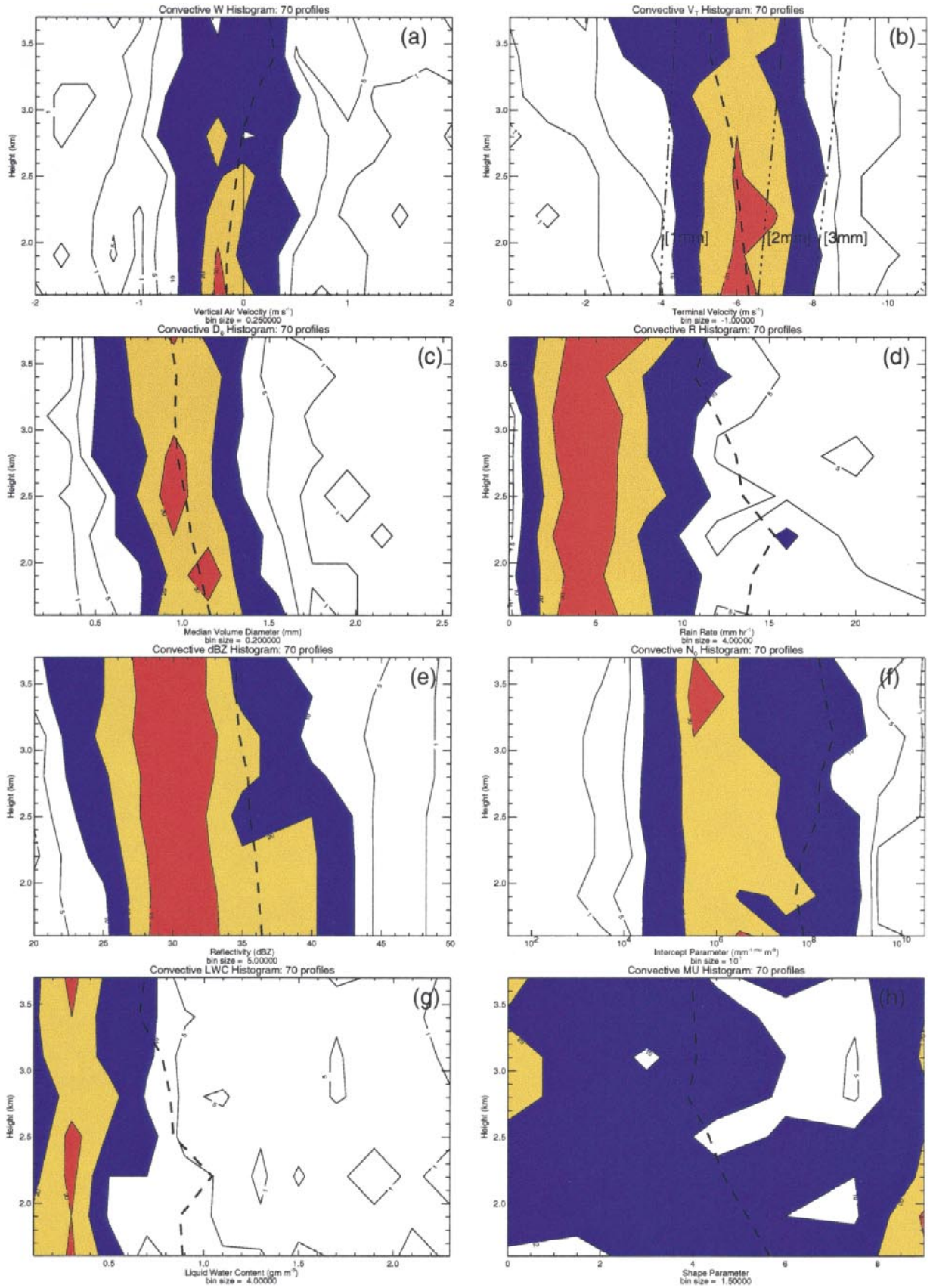

FIG. 5. Same as Fig. 4 but for the convective precipitation category.

er because of the differences in shape between the convective and stratiform parameter distributions. The convective category has a larger number of R and Z values at the high end. These relatively infrequent occurrences of R and Z produce a pronounced separation of the convective mean and mode compared to the stratiform distributions. The upward decrease in the mean convective reflectivity ($\sim$1 dB km^{-1}) is consistent with many previous studies of tropical oceanic MCSs using scanning radar (e.g., Szoke et al. 1986) and profiler (e.g., Williams et al. 1995) data. The consequences of different R and Z parameter distributions in stratiform and convective rain are discussed below in section 3e. A similar effect also occurs in the convective LWC (Fig. 5g). This plot indicates that the liquid water concentration can exceed 2 gm m^{-3} in the convective cores of these MCSs. These values, however, are not unreasonable based on in situ aircraft observations of Florida thunderstorms (Willis et al. 1994).

Comparison of the retrieved N_0 distributions between convective (Fig. 5f) and stratiform (Fig. 4f) shows that the mode of the convective N_0 distribution is about one order of magnitude higher than the corresponding stratiform distribution. This results supports a number of studies using surface-based spectrometers and disdrometers that have shown a systematic decrease in the intercept parameter N_0 as precipitation changed from convective to stratiform (e.g., Waldvogel 1974; Tokay et al. 1995; Tokay and Short 1996). The convective μ distribution (Fig. 5h) shows significantly more variability in comparison with the stratiform μ, although the mean profiles are similar. The wide variation of μ is most likely a consequence of this parameter's sensitivity to errors in the vertical air motion retrieval (McKague et al. 1998). Taken together, the convective parameter distributions show a more complicated vertical structure in comparison with the stratiform category. For the most part, the convective drop-size distributions have smaller D_0 and V_T and larger R, LWC, Z, and N_0, in agreement with previous comparisons of convective and stratiform drop-size distributions.

The parameter distributions for the mixed category are shown in Fig. 6. The drop-size distribution parameter values in Fig. 6 are intermediate between the convective and stratiform results. Recall that the classification scheme in this study utilizes fall speed and spectral width characteristics from the UHF and VHF profilers but does not incorporate any information on rainfall rate or reflectivity gradients as used in other classification schemes. Comparison of Figs. 4, 5, and 6 suggests that the classification algorithm produces results that are microphysically consistent with the lifecycle evolution of the MCSs.

e. Reflectivity–rainfall relations

In this section, we use the profiler-retrieved drop-size distribution characteristics to develop Z–R relations in each precipitation category. Figure 7 shows the mean profiles of reflectivity (Z) and rainfall (R) for each precipitation category as a function of height. It can be seen that the mean rain rate between precipitation categories varies by over a factor of 3 while the reflectivities are within about four dB. That is, the figure suggests that, *for a given reflectivity,* there is a significant increase in the rain rate as the precipitation category changes from stratiform to convective. This suggests that different Z–R relations occur for each precipitation regime. The differences in expected rain rate for convective and stratiform precipitation can be illustrated another way. Using reflectivity values from Fig. 7 for the convective and stratiform precipitation categories, it is possible to calculate the expected rain rate with the commonly used NEXRAD Z–R relation

$$Z = 300R^{1.4}. \tag{5}$$

Following this procedure for the stratiform category ($Z = 31.5$ dBZ) yields a rainfall rate of 3 mm h^{-1}, very close to the observed mean value of about 4 mm h^{-1} (Fig. 7b). With Eq. (5) for convective rain, however, the reflectivity value from Fig. 7 ($Z = 36$ dBZ) underestimates the retrieved rain rate by more than a factor of 2.

In order to explore more fully the differences in Z–R parameterizations by precipitation regime, Z–R relationships were determined for each precipitation category in the 1.6–3.7 km height range using a linear regression fit that minimizes the χ^2 error statistic (in log–log space) to the equation

$$Z = AR^B. \tag{6}$$

Plots of the vertical structure and variability of the coefficient A and exponent B parameters are shown in Fig. 8. There is a general trend for A to increase with decreasing height without much change in B in all three precipitation regimes. The trend in coefficient A with height is particularly pronounced for the convective and stratiform categories. In the stratiform region, the coefficient A increases by $\sim$37% with decreasing height. Exponent B also decreases slightly in the stratiform category. The combined signature of A increasing and B decreasing is consistent with the expected change in Z–R due to one or more of the following: coalescence, evaporation, or size sorting (Gunn and Marshall 1955; Atlas and Chmela 1957; Wilson and Brandes 1979; Ulbrich and Atlas 1998). As pointed out by Atlas et al. (1999), size sorting from wind shear effects should not alter the Z–R relation provided that a sufficient number of samples are collected. This is because sorting will affect both ends of the drop-size distribution for a sufficiently large sample population. Recall that the stratiform category consists of over 400 stacked spectra profiles so that size sorting is not expected to play a significant role in producing the changes in Z–R observed with height in the stratiform category. The profiler observations cannot quantify the contribution of coalescence and evaporation to the drop-size distribution; however,

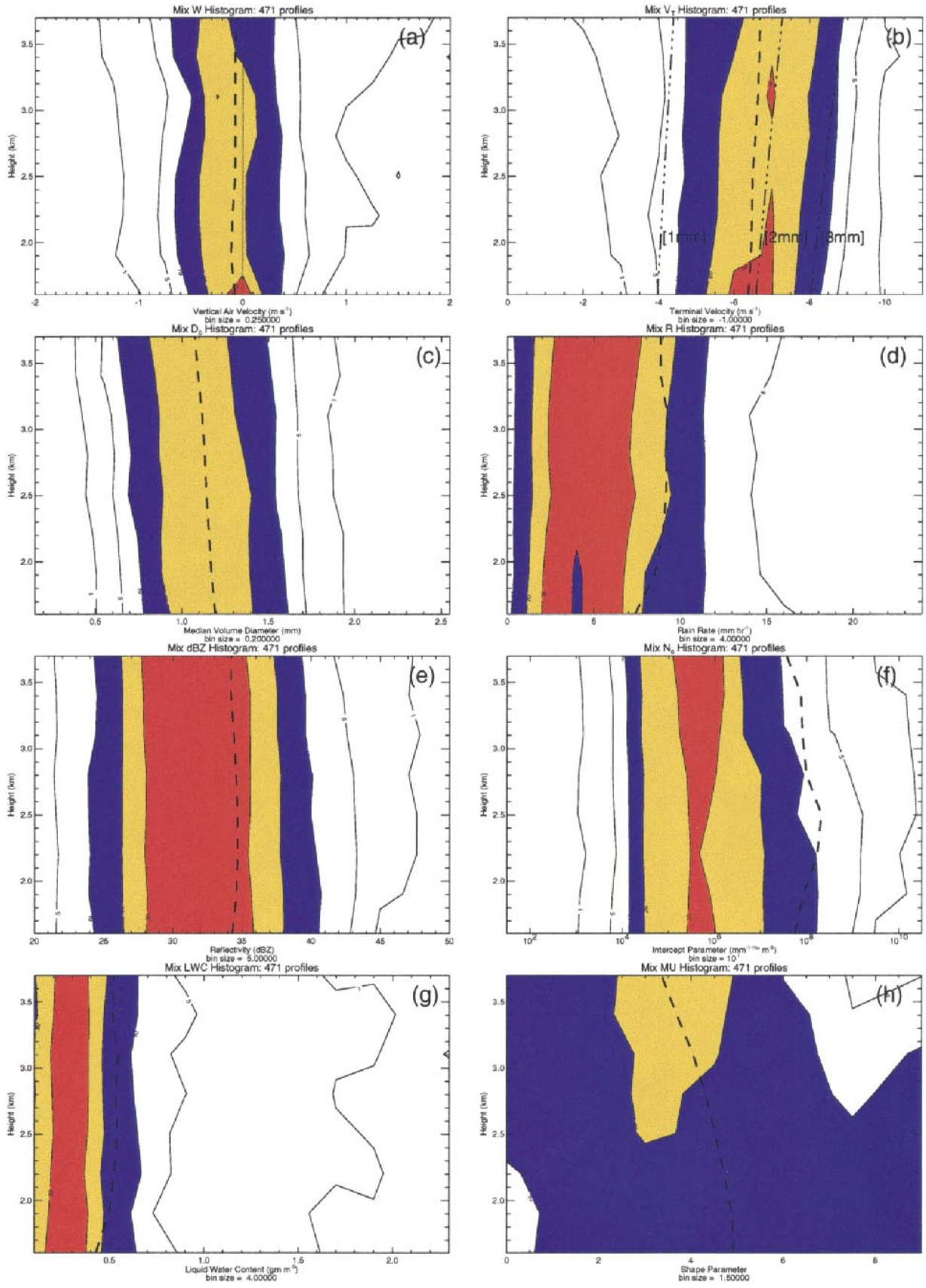

FIG. 6. Same as Fig. 4 but for the mixed precipitation category.

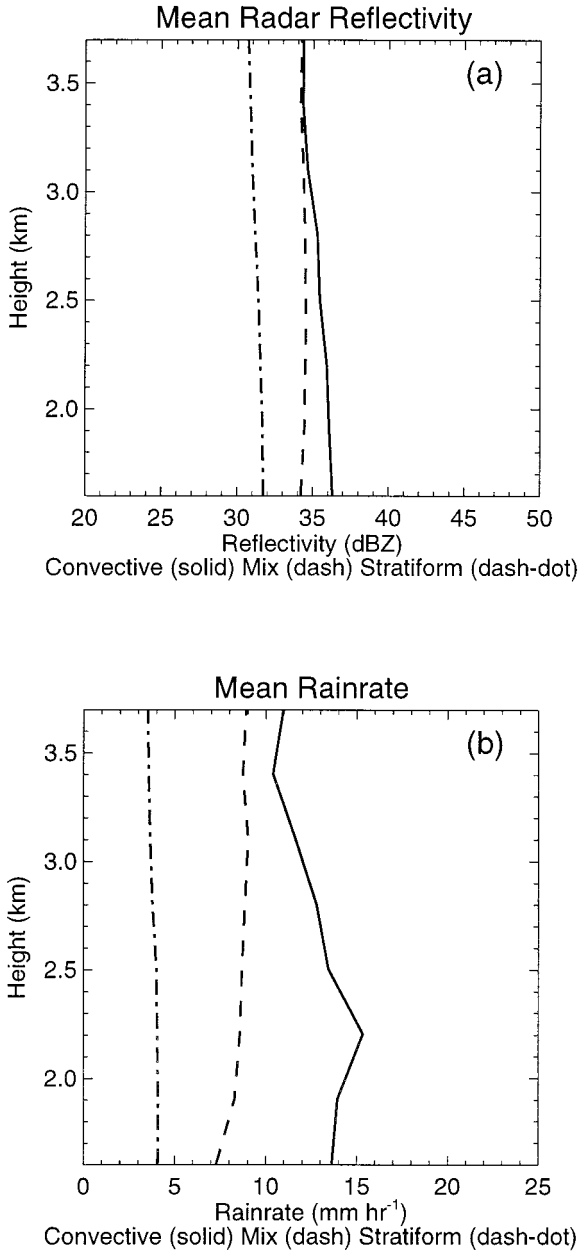

FIG. 7. Mean profiles of (a) radar reflectivity and (b) rain rate for the convective (solid line), mixed (dash line), and stratiform (dash-dot line) precipitation categories. The mean profiles are the same as in Figs. 4, 5, and 6.

the fact that the parameter distribution results in Fig. 4 indicate nearly constant R, LWC, and Z with height suggests that evaporation must be nearly balanced by coalescence in these events for the height range used in the analysis.

The coefficient and exponent values shown in Fig. 8 can be compared with corresponding ground-based disdrometer measurements collected during the 1993/94 wet season and analyzed by Tokay et al. (1995)[5]. Although the disdrometer data in the Tokay et al. analysis were available only for the latter part of the 1993/94 wet season, it did sample several events used in this study (i.e., 94046 and 94056) and can therefore provide a measure of validation for the profiler Z–R relations shown in Fig. 8. The convective and stratiform values of A at the lowest height (1.6 km) are 177 and 306, respectively. These are in good agreement with the corresponding ground-based disdrometer A values of 175 (convective) and 335 (stratiform) derived in the Tokay et al. study using 1-min-averaged data. The agreement between the profiler and disdrometer measurements is encouraging, especially when considering the large difference in height (1.6 km) and space (40 km) between the instruments as well as the fact that many events were not simultaneously sampled by each instrument. Note, however, that the exponent B values are somewhat higher in the Tokay et al. disdrometer study (1.37 versus $\sim$1.05 in this study). The fact that B is close to 1.0 for all three precipitation regimes implies a nearly constant value of the mass-weighted diameter (Atlas et al. 1999). These results are consistent with in situ aircraft measurements collected in TOGA COARE (Ulbrich and Atlas 1998).

The convective profiles of coefficient A and exponent B show more vertical structure than in the stratiform region, probably as a result of the much lower number of spectra in this category as well as from the large variability in the convective drop size distributions (Fig. 5). There is a general trend for A to increase with decreasing height ($\sim$78%) similar to the stratiform profile. For the most part, the convective coefficient A is approximately a factor of 2 lower than the stratiform A coefficient for all heights. These results are consistent with Huggel et al. (1996) who argued that convective precipitation is dominated by small particles (relative to stratiform precipitation with a pronounced brightband signature) and produces rain rates that are larger than predicted with a standard Z–R such as Eq. (5). Note that there is a small reversal of the trend for the convective A to increase downward in two layers: 3.1–2.8 km and below 1.9 km. In these same layers, exponent B increases slightly. The combined effect (decrease in A and increase in B) is expected from accretion of cloud particles (Atlas and Chmela 1957; Wilson and Brandes 1979).

The mixed category profiles (Fig. 8) show similar features with the stratiform results above 2.2 km; however, below this height, the combined signature of A and B suggests accretion, similar to the convective category. In this case, the relative change in A with height is much smaller than for the stratiform or convective categories.

[5] Two separate impact disdrometers were deployed near Darwin during the 1993/94 wet season. One was located 3.5 km from the profiler site (discussed in section 3c), and the other was located near Humpty Doo ($\sim$40 km from the profilers discussed in this section).

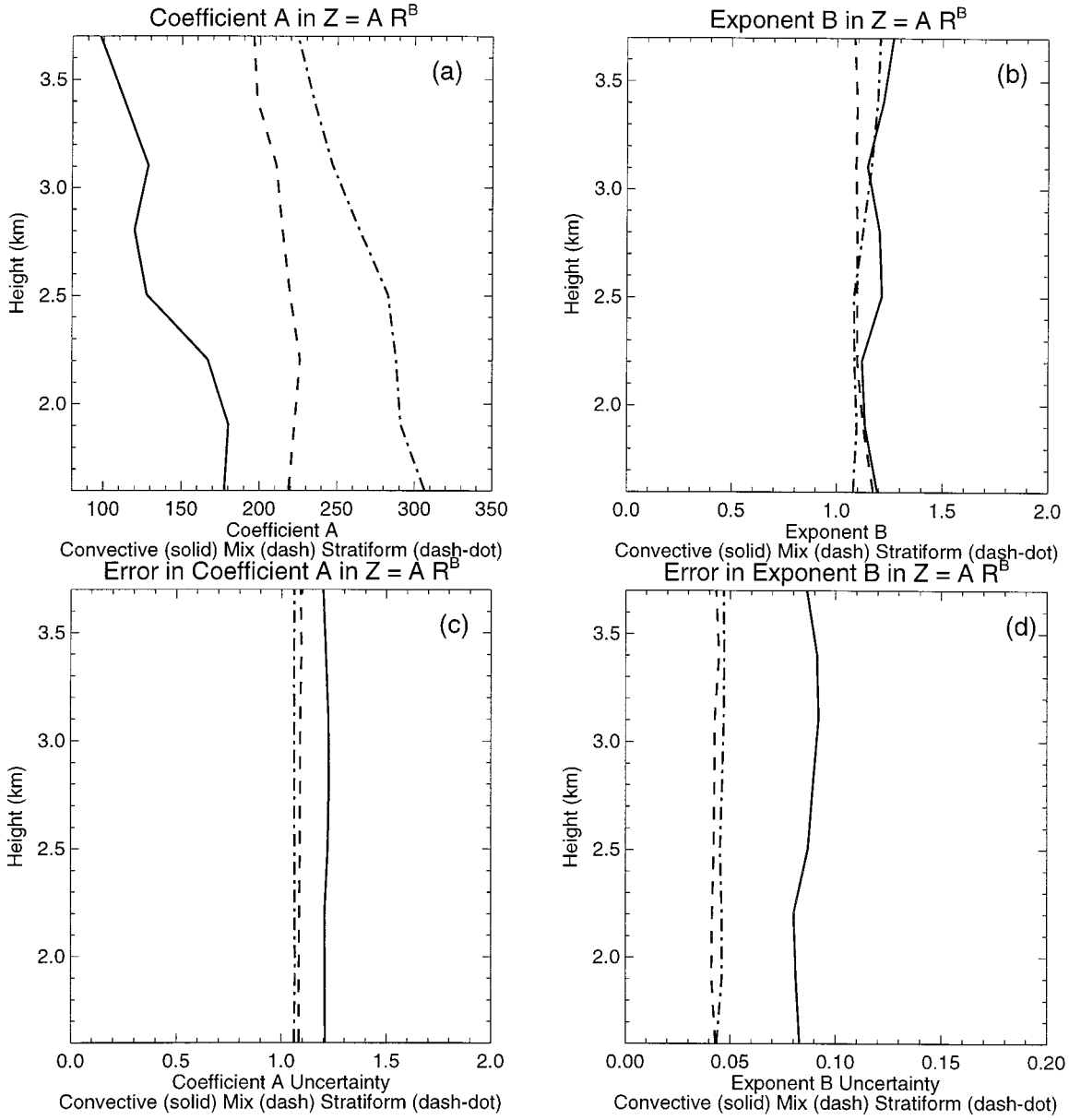

FIG. 8. Vertical profiles of (a) coefficient *A* and (b) exponent *B* for the convective (solid line), mixed (dash line), and stratiform (dash–dot line) precipitation categories. The profiles were derived using a linear regression procedure which minimizes the χ^2 statistic in log space. The standard errors of the fit for coefficient *A* and exponent *B* determined from the linear regression are shown in (c) and (d), respectively.

In order to provide more insight into the differences in the convective and stratiform *Z–R* relations as a function of height, the best-fit regressions for two selected reflectivities (30 and 40 dB*Z*) were compared, and the results are shown in Fig. 9. Note that the profiles in Fig. 9 are not constant, because of the change in slope of the *Z–R* relation with height in each precipitation regime. Figure 9 indicates that there can be large differences in the convective and stratiform rain rates (~15%–85%) for a given reflectivity and emphasizes the fact that the *Z–R* relation varies, not only by precipitation category, but also as a function of height.

4. Conclusions

A dual-frequency profiler retrieval method is used to examine the differences in the drop-size distribution from a total of eight MCSs occurring near Darwin, Northern Territory, Australia. The profiler retrievals were divided into three categories of rainfall (convec-

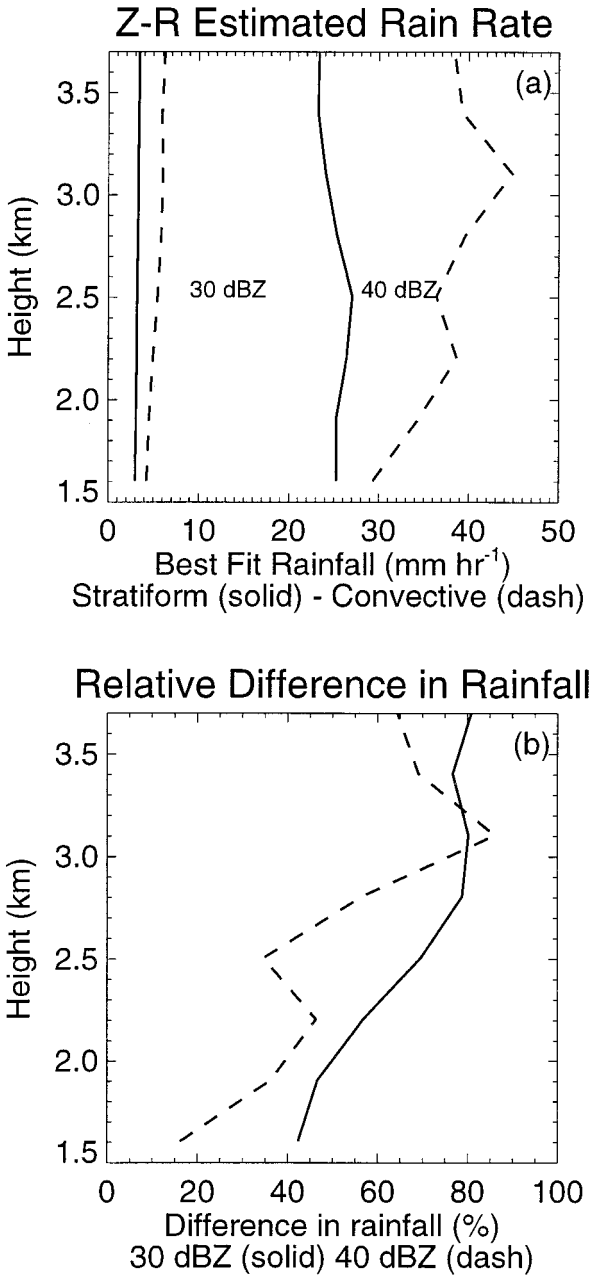

FIG. 9. (a) Best-fit estimate of convective (solid line) and stratiform (dashed line) rain rate using the *Z–R* relations shown in Fig. 8 for *Z* = 30 and 40 dBZ. (b) Percent difference in rain rate between convective and stratiform [(convective–stratiform)/stratiform] as a function of height using the best-fit *Z–R* relations for two selected reflectivities: 30 dB*Z* (solid) and 40 dB*Z* (dashed).

tive, mixed, and stratiform) as a function of height, based on a modified version of Williams et al. (1995). The modification includes information on turbulence in the precipitation discrimination routine. The method does not incorporate rainfall or reflectivity parameters. It is found to produce reasonable profiles/distributions of these parameters based on comparisons with previous results.

Statistical analyses were performed for each category of data using a relatively rigid set of criteria to ensure that only the most reliable retrievals were included. The criteria were found to have minimal effect in the mixed and stratiform categories; however, the procedure probably limited the number of intense convective samples and biased this category toward weak convection. The results showed that, because of the relatively large amount of high-frequency variability in each precipitation category (especially convective), the modes of the drop-size distribution parameters displayed only small variation among precipitation categories as a function of height. However, the mean profiles displayed pronounced differences caused by the increasing skewness of each parameter distribution as the precipitation changed from stratiform to convective. The skewness was caused by the more frequent occurrence of values at the high end for any given parameter in the convective category. These differences in the mean profiles have important implications for rainfall reflectivity relationships.

The *Z–R* relations were derived as a function of height in each precipitation category. Similar to results from a number of previous studies, the rain rate increased from stratiform to convective precipitation *for a given reflectivity*; however, the magnitude of this change was observed to depend on both rain rate and height. In all three categories, the coefficient *A* was found to increase with decreasing height over the depth of the analysis; however, there were small reversals to this trend in the convective and mixed categories. The exponent *B* slightly decreased with height (stratiform), remained nearly constant (convective), or increased slightly (mixed). The variability of exponent *B* was minimal in comparison with coefficient *A*. The overall increase in *A* and decrease in *B* in stratiform precipitation is consistent with one or more of the following: size sorting, evaporation, or coalescence growth. Given the relatively large number of analyzed stratiform retrievals, size sorting is not expected to play a major role in modifying the overall shape of any of the stratiform parameter distributions. Although the profiler observations cannot quantify the contribution of each microphysical process, the vertical structure of the stratiform drop-size distribution parameters suggest an equilibrium between coalescence and evaporation over the height range examined in these MCSs. The behavior of the drop-size distribution parameters in the mixed and convective categories was more complicated, because of the more heterogeneous character of these precipitation categories (as evidenced by vertical air motion structure).

Comparison of the *Z–R* relations in each category of data showed that the difference in rainfall between convective and stratiform (at a given reflectivity) can be substantial, ranging from 15%–85% in the height range of the analysis. These results emphasize that, despite

overlap in the convective and stratiform drop-size parameter distributions, there can be important differences between the two regimes that are manifested in the estimation of rainfall. Furthermore, these differences have important consequences for *Z–R* parameterizations.

Future efforts should be directed toward using the profiler data to develop climatologies of *Z–R* relations in different geographical regions and testing the robustness of these relationships with scanning radar and rain gauge data. The profiler observations could also be used in conjunction with a numerical cloud model to examine the model sensitivity (in terms of downdraft intensity and latent heating response) to the parameterized drop-size distribution. Finally, improvements should be made in the drop-size distribution retrieval process using wind profilers. By extending the range of the retrieval methodology (both closer to ground surface and above the freezing level), more of the precipitation vertical structure can be revealed. This information could provide improved validation of rainfall and radiative heating calculations for both surface and satellite-based sensors.

Acknowledgments. Support for this work was provided by a CIRES Visiting Fellowship and NASA Grant NAGW 4146. The first author is also grateful to Mr. Otto Thiele in the TRMM office at NASA GSFC for supporting this research effort. Appreciation is extended to Drs. David Atlas, David Short, and Ali Tokay for their constructive comments on this work. The reviewers also provided helpful suggestions to improve the manuscript. Darren McKague provided the disdrometer data. This work is dedicated to the memory of Dr. Deepak Rajopadhyaya.

REFERENCES

Atlas, D., and A. C. Chemela, 1957: Physical-synoptic variations of raindrop size parameters. *Proc. Sixth Weather Radar Conf.,* Cambridge, MA, Amer. Meteor. Soc., 21–29.

——, R. S. Srivastava, and R. S. Sekhon, 1973: Doppler radar characteristics of precipitation at vertical incidence. *Rev. Geophys. Space Sci.,* **11,** 1–35.

——, P. Willis, and F. Marks, 1995: The effect of convective updrafts and downdrafts on reflectivity–rain rate relations and water budgets. Preprints, *27th Int. Conf. on Radar Meteorology*, Vail, CO, Amer. Meteor. Soc., 19–22.

Atlas, D., C. W. Ulbrich, F. D. Marks Jr., E. Amitai, and C. R. Williams, 1999: Systematic variation of drop size and radar–rainfall relations. *J. Geophys. Res.,* **104,** 6155–6169.

Austin, P. M., 1987: Relation between measured radar reflectivity and surface rainfall. *Mon. Wea. Rev.,* **115,** 1053–1070.

Battan, L. J., 1973: *Radar Observations of the Atmosphere.* University of Chicago Press, 324 pp.

Beard, K. V., 1985: Simple altitude adjustments to raindrop velocities for Doppler radar analysis. *J. Atmos. Oceanic Technol.,* **2,** 468–471.

Carter, D. A., K. S. Gage, W. L. Ecklund, W. M. Angevine, P. E. Johnston, A. C. Riddle, J. S. Wilson, and C. R. Williams, 1995: Developments in UHF lower tropospheric wind profiling at NOAA's Aeronomy Laboratory. *Radio Sci.,* **30,** 977–1001.

Chandrasekar, V., and V. N. Bringi, 1987: Simulation of radar reflectivity and surface measurements of rainfall. *J. Atmos. Oceanic Technol.,* **4,** 464–478.

Cifelli, R., and S. A. Rutledge, 1998: Vertical motion, diabatic heating, and rainfall characteristics in north Australia convective systems. *Quart. J. Roy. Meteor. Soc.,* **124,** 1133–1162.

Currier, P. E., S. K. Avery, B. B. Balsley, and K. S. Gage, 1992: Use of two wind profilers for precipitation studies. *Geophys. Res. Lett.,* **19,** 1017–1020.

Ferrier, B. S., W. K. Tao, and J. Simpson, 1995: A double-moment multiple-phase four-class bulk ice scheme. Part II: Simulations of convective storms in different large-scale environments and comparisons with other bulk parameterizations. *J. Atmos. Sci.,* **52,** 1001–1033.

——, J. Simpson, and W. K. Tao, 1996: Factors responsible for precipitation efficiencies in midlatitude and tropical squall simulations. *Mon. Wea. Rev.,* **124,** 2100–2125.

Gossard, E. E., 1988: Measuring drop-size distributions in clouds with a clear-air sensing Doppler radar. *J. Atmos. Oceanic Technol.,* **5,** 640–649.

Gunn, K. L. S., and J. S. Marshall, 1955: The effect of wind shear on falling precipitation. *J. Meteor.,* **12,** 339–349.

Houze, R. A., Jr., 1989: Observed structure of mesoscale convective systems and implications for large-scale heating. *Quart. J. Roy. Meteor. Soc.,* **115,** 425–461.

Huggel, A., W. Schmid, and A. Waldvogel, 1996: Raindrop size distributions and the radar bright band. *J. Appl. Meteor.,* **35,** 1688–1701.

Joss, J., and A. Waldvogel, 1967: Ein Spektrograph fur Niedersclagstropfen mit automatischer Auswertung (in German). *Pure Appl. Geophys.,* **68,** 240–246.

Maguire, W. B., II, and S. K. Avery, 1994: Retrieval of raindrop size distributions using two Doppler wind profilers: Model sensitivity testing. *J. Appl. Meteor.,* **33,** 1623–1635.

Mapes, B., and R. A. Houze Jr., 1993: An integrated view of the 1987 Australian monsoon and its mesoscale convective systems. II: Vertical structure. *Quart. J. Roy. Meteor. Soc.,* **119,** 733–754

——, and ——, 1995: Diabatic divergence profiles in western Pacific mesoscale convective systems. *J. Atmos. Sci.,* **52,** 1807–1828.

May, P. T., and D. K. Rajopadhyaya, 1996: Wind profiler observations of vertical motion and precipitation microphysics of a tropical squall line. *Mon. Wea. Rev.,* **124,** 621–633.

——, and ——, 1997: Corrigendum. *Mon. Wea. Rev.,* **125,** 410–413.

——, and ——, 1999: Vertical velocity characteristics of deep convection over Darwin, Australia. *Mon. Wea. Rev.,* **127,** 1056–1071.

McGaughey, G., E. J. Zipser, R. W. Spencer, and R. E. Hood, 1996: High-resolution passive microwave observations of convective systems over the tropical Pacific Ocean. *J. Appl. Meteor.,* **35,** 1921–1947.

McKague, D., K. F. Evans, and S. K. Avery, 1998: Assessment of the effects of drop size distribution variations retrieved from UHF radar on passive microwave remote sensing of precipitation. *J. Appl. Meteor.,* **37,** 155–165.

Rajopadhyaya, D. K., P. T. May, and R. A. Vincent, 1993: A general approach to the retrieval of rain drop-size distributions from VHF wind profiler Doppler spectra: Modeling results. *J. Atmos. Oceanic Technol.,* **10,** 710–717.

——, ——, R. Cifelli, S. K. Avery, C. R. Williams, W. L. Ecklund, and K. S. Gage, 1998: The effect of vertical air motions on rain rates and median volume diameter determined from combined UHF and VHF wind profiler measurements and comparisons with rain gauge measurements. *J. Atmos. Oceanic Technol.,* **15,** 1306–1319.

Ralph, F. M., 1995: Using radar-measured radial vertical velocities to distinguish precipitation scattering from clear-air scattering. *J. Atmos. Oceanic Technol.,* **12,** 257–267.

Richter, C., and M. Hagen: 1997: Drop-size distributions of raindrops by polarization radar and simultaneous measurements with disdrometer, wind profiler and PMS probes. *Quart. J. Roy. Meteor. Soc.,* **123,** 2277–2296.

Rogers, R. R., 1967: Doppler radar investigation of Hawaiian rain. *Tellus,* **19,** 432–455.

——, D. Baumgardner, S. A. Ether, D. A. Carter, and W. L. Ecklund, 1993: Comparison of raindrop size distributions measured by radar wind profiler and by airplane. *J. Appl. Meteor.,* **32,** 694–699.

Short, D. A., T. Kozu, and K. Nakamura, 1990: Rainrate and raindrop size distribution observations in Darwin, Australia. *Proc. URSI Commission F Open Symp. on Regional Factors in Predicting Radiowave Attenuation Due to Rain,* Rio de Janeiro, Brazil, International Union of Radio Science Commission, 35–40.

Simpson, J., R. F. Adler, and G. R. North, 1988: A proposed Tropical Rainfall Measuring Mission (TRMM) satellite. *Bull. Amer. Meteor. Soc.,* **69,** 278–295.

Steiner, M., and R. A. Houze Jr., 1997: Sensitivity of the estimated monthly convective rain fraction to the choice of *Z–R* relation. *J. Appl. Meteor.,* **36,** 452–462.

Szoke, E. J., E. J. Zipser, and D. P. Jorgensen, 1986: A radar study of convective cells in mesoscale systems in GATE. Part I: Vertical profile statistics and comparison with hurricanes. *J. Atmos. Sci.,* **43,** 182–197.

Tokay, A., and D. A. Short, 1996: Evidence from tropical raindrop spectra of the origin of rain from stratiform versus convective clouds. *J. Appl. Meteor.,* **35,** 355–371.

——, ——, and B. Fisher, 1995: Convective versus stratiform precipitation classification from surface measured drop size distributions at Darwin, Australia, and Kapingamarangi atoll. Preprints, *27th Int. Conf. on Radar Meteorology,* Vail, CO, Amer. Meteor. Soc., 690–693.

——, ——, C. R. Williams, E. L. Ecklund, and K. S. Gage, 1999: Tropical rainfall associated with convective and stratiform clouds: Intercomparison of disdrometer and profiler measurements. *J. Appl. Meteor.,* **38,** 302–320.

Ulbrich, C. W., 1983: Natural variations in the analytical form of the raindrop size distribution. *J. Climate Appl. Meteor.,* **22,** 1764–1775.

——, and D. Atlas, 1998: Rainfall microphysics and radar properties: Analysis methods for drop size spectra. *J. Appl. Meteor.,* **37,** 912–923.

Viltard, N., E. Obligis, V. Marecal, and C. Klapisz, 1998: Retrieval of precipitation from microwave airborne sensors during TOGA COARE. *J. Appl. Meteor.,* **37,** 701–716.

Wakasugi, K., A. Mizutani, M. Matsuo, S. Fukao, and S. Kato, 1986: A direct method for deriving drop-size distribution and vertical air velocities from VHF Doppler radar spectra.. *J. Atmos. Oceanic Technol.,* **3,** 623–629.

Waldvogel, A., 1974: The N_0 jump in raindrop spectra. *J. Atmos. Sci.,* **31,** 1067–1078.

Williams, C. R., W. L. Ecklund, and K. S. Gage, 1995: Classification of precipitating clouds in the tropics using 915-MHz wind profilers. *J. Atmos. Oceanic Technol.,* **12,** 996–1012.

Willis, P. T., J. Hallett, R. A. Black, and W. Hendricks, 1994: An aircraft study of rapid precipitation development and electrification in a growing convective cloud. *Atmos. Res.,* **33,** 1–24.

Wilson, J. W., and E. A. Brandes, 1979: Radar measurement of rainfall—A summary. *Bull. Amer. Meteor. Soc.,* **60,** 1048–1058.

Yuter, S. E., and R. A. Houze Jr., 1995: Three-dimensional kinematic and microphysical evolution of Florida cumulonimbus. Part II: Frequency distributions of vertical velocity, reflectivity, and differential reflectivity. *Mon. Wea. Rev.,* **123,** 1941–1963.

——, and ——, 1997: Measurements of raindrop size distributions over the Pacific warm pool and implications for *Z–R* relations. *J. Appl. Meteor.,* **36,** 847–867.

Zawadzki, I., 1984: Factors affecting the precision of radar measurements of rain. Preprints, *22d Int. Conf. on Radar Meteorology,* Zurich, Switzerland, Amer. Meteor. Soc., 251–256.